

# A model for the X-ray absorption in Compton-thin AGN

A. Lamastra, G. C. Perola, and G. Matt

Dipartimento di Fisica “E. Amaldi”, Università degli Studi Roma Tre, via della Vasca Navale 84, 00146 Roma, Italy  
e-mail: lamastra@fis.uniroma3.it

Received 9 August 2005 / Accepted 30 November 2005

## ABSTRACT

The fraction of AGN with photoelectric absorption in the X-rays ranging from  $N_{\text{H}}$  of  $10^{22}$  up to about  $10^{24}$   $\text{cm}^{-2}$  (Compton-thin) appears observationally to be anticorrelated to their luminosity  $L_x$ . This recently found evidence is used to investigate the location of the absorbing gas. The molecular torus invoked in the unified picture of AGN, while it can be regarded as confirmed on several grounds to explain the Compton-thick objects, do not conform to this new constraint, at least in its physical models as developed so far. In the frame of observationally based evidence that in Compton-thin sources the absorbing gas might be located far away from the X-ray source, it is shown that the gravitational effects of the black hole (BH) on the molecular gas in a disk, within 25–450 pc (depending on the BH mass, from  $10^6$  to  $10^9 M_{\odot}$ ), leads naturally to the observed anticorrelation, under the assumption of a statistical correlation between the BH mass and  $L_x$ . Its normalization is also reproduced provided that the surface density,  $\Sigma$ , of this gas is larger than about 150–200  $M_{\odot} \text{pc}^{-2}$ , and assuming that the bolometric luminosity is one tenth of the Eddington limit. Interestingly, the required values are consistent with the value of the 300 pc molecular disk in our own galaxy, namely 500  $M_{\odot} \text{pc}^{-2}$ . In a sample of nearby galaxies from the BIMA SONG survey, it is found that half of the objects have central  $\Sigma$  larger than 150  $M_{\odot} \text{pc}^{-2}$ . Given the simplicity of the proposed model, this finding is very encouraging, waiting for future higher resolution surveys in CO on more distant galaxies.

**Key words.** galaxies: active – X-rays: galaxies – ISM: clouds

## 1. Introduction

Similar to dust extinction in the optical, photoelectric absorption in X-rays provides clues on the environment of Active Galactic Nuclei (AGN). In general the latter provides information which is more straightforward to interpret than the former, because it depends a) on atomic properties and consequently only on the chemical composition of the medium, b) on the adoption of a shape for the X-ray continuum, which is empirically known to follow a simple Power Law (PL). The values of the spectral photon index,  $\Gamma$ , display a rather modest dispersion (e.g. Perola et al. 2002; Piconcelli et al. 2005); furthermore, in any single object under consideration, and provided that the absorption is Compton-thin (i.e. with  $N_{\text{H}}$  not exceeding  $\sigma_{\text{Th}}^{-1} = 1.5 \times 10^{-24} \text{cm}^{-2}$ ), the exact value of  $\Gamma$  can be directly measured, given an adequately wide observational band and sufficient statistics for the spectral counts. Here, though, it is more important to stress the limitations, which are mainly of three sorts:

1. The source of the PL photons is, for most practical purposes, point-like, and therefore it remains questionable how to relate the total absorbing matter density (the absorbing column  $N_{\text{H}}$ ) to bi-dimensional information (either direct or indirect) on the circumnuclear matter from observations in other wave-bands. In other words, usually it cannot be excluded that the observed column might be pertaining to that

unique line of sight, rather than to the overall configuration of the circumnuclear matter.

2. While it is spectroscopically possible (as amply demonstrated even before the use of very high resolution instruments) to disentangle the imprints of a multi-phase (in ionization terms) absorber, it is by no means immediately possible to recover the space distribution of the phases along the line of sight. When the ionization is attributed to the photoelectric effects of the PL source as a reasonable hypothesis (better still when it can be observationally proven not to be of collisional origin), it is generally regarded as most likely that the high ionization gas is very close to the centre. This leaves however quite open the possibility that the low (in practice, indistinguishable from neutral) ionization gas might lie either much further away or equally close but dense enough to remain neutral.
3. When  $N_{\text{H}}$  is larger than about  $10^{24} \text{cm}^{-2}$ , the column is Compton-thick, that is a diffusive process adds to the absorption process to deplete the specific intensity along the line of sight. A truly thick absorber ( $\tau_{\text{Th}} \gg 1$ ) reduces the intensity by several orders of magnitude all the way throughout the hard X-ray band, and renders in fact its quantitative evaluation impossible, except for a “lower limit” (e.g. Matt et al. 1999).

It must be emphasized that, in general, AGN spectra contain another component in addition to the PL, which becomes

evident beyond 8–10 keV. It is due to reflection from Compton-thick, neutral gas, and, as expected on physical grounds, it is accompanied by a strong fluorescent iron line. From a pure observational point of view, this component is often the only visible one below  $\sim 10$  keV when the PL is photoelectrically absorbed by  $N_{\text{H}}$  of about  $10^{24}$  cm $^{-2}$  (corresponding to a turnover in energy at about 10 keV), or greater. Its intensity is typically a few percent of the primary one in the 2–10 keV band. In such systems, it is regarded as very reasonable to assume that the absorbing and the reflecting gas belong to one and the same circumnuclear structure. Historically, it was the spectropolarimetric measurements in the optical band of NGC 1068 which led Antonucci & Miller (1985) to propose the so-called “unified model”. This model (Antonucci 1993) envisages the existence of a thick and dusty “torus” of molecular gas around the nucleus, extending out to a few tens of pc at most (Risaliti et al. 1999) and with a substantial covering factor to account for the large ratio of type 2 to type 1 Seyferts, at least in the local Universe (4:1, if also Seyfert 1.8 and 1.9 are included: Maiolino & Rieke 1995; Ho et al. 1997; it is worth recalling that the local Universe is dominated by relatively low luminosity objects as compared to the Quasi Stellar Objects, QSO). In its basic form, the model has been widely confirmed, most notably by measurements in the hard X-ray band, which showed that most type 2 Seyferts are X-ray absorbed. The situation, however, is likely to be more complex than the zero-th order model would predict. On one hand, there is increasing evidence of a substantial population of optically inactive, obscured AGN, both in the local (Maiolino et al. 2003) and more distant (Comastri et al. 2002; Brandt & Hasinger 2005) Universe. This implies that the ratio between X-ray obscured to unobscured AGN may be larger than that between type 2 and type 1 Seyferts. On the other hand, other absorbing regions, besides the torus, may exist in the complex environment of AGN: dust lanes (Malkan et al. 1998), starburst regions (Weaver 2002), the galactic disk (Maiolino & Rieke 1995). Indeed, it has been suggested (see e.g. Matt 2000, 2004, and references therein) that Compton-thick absorption (which, in the local Universe, is observed in about half of optically selected type 2 Seyferts, Risaliti et al. 1999; Guainazzi et al. 2005, the percentage rising when “elusive” AGN are also taken into account, Maiolino et al. 2003) is related to the torus, while Compton-thin absorption is due to one (or more) of the other possible absorbing regions. (If a dust/gas ratio typical of the cold interstellar medium of our Galaxy is adopted, Compton-thin absorption, i.e.  $N_{\text{H}}$  in the  $10^{22}$ – $10^{24}$  cm $^{-2}$  range, is sufficient to explain the extinction of the BLR lines).

This paper will address the question of the location of the absorber in the light of new results from X-ray surveys in the 2–10 keV band. The sensitivity reached in this band with the XMM-Newton and Chandra satellites made it, for the first time, possible to study AGN of both type 1 and 2, with sufficient statistics to investigate the  $N_{\text{H}}$  distribution as a function of the intrinsic (PL) luminosity and of the cosmic epoch out to  $z$  about 4.

Surveys limited to 10 keV on the high energy side (and with instrument sensitivity dropping rapidly beyond 5–7 keV) are doomed to miss almost completely the Compton-thick

objects. Thus the results must be read as pertinent, among the AGN classified through optical spectroscopy as type 2, only to those with  $N_{\text{H}}$  less than  $10^{24}$  cm $^{-2}$ . Basically, the question addressed in this paper is whether the new results can be understood in the context of the unified model based on just one element, the torus mentioned above, or, if not, if one can conceive of just one realistic (astrophysically) additional element able to provide a positive answer, with the least possible number of assumptions. In particular, the new contribution of this paper is the use of one further constraint, namely the decrease of the fraction of Compton-thin obscured AGN with increasing X-ray luminosity, an anticorrelation which have recently emerged from the statistical analysis of the abovementioned types of survey (Ueda et al. 2003; Hasinger 2004; La Franca et al. 2005).

In Sect. 2 this new constraint is described. In Sect. 3 the current physical models of the torus are discussed and shown to be unable to account, even qualitatively, for the anticorrelation. In Sect. 4 it is shown that, if the obscuration is due to molecular gas in galactic disks, then the gravitational effects of the black hole on its spatial distribution within 25–450 pc (depending on the mass) leads naturally to an anticorrelation. An encouragingly reasonable quantitative match is achieved under two conditions: that the molecular mass surface density exceeds  $\sim 150 M_{\odot}$  pc $^{-2}$  within 25–450 pc, and that in a statistical sense the bolometric luminosity is proportional to the black hole mass, and equal to about 10% of the Eddington luminosity. In Sect. 5 these two conditions are discussed in the light of the evidence available, and a positive conclusion is drawn.

## 2. A new observational constraint: the luminosity-absorption anticorrelation

A statistical investigation on the photoelectric absorption properties of Compton-thin AGN was first obtained, down to a flux limit  $F(2\text{--}10\text{ keV})$  of about  $10^{-13}$  erg cm $^{-2}$  s $^{-1}$  (which corresponds to about 25% of the X Ray Background, XRB) with imaging instruments operating up to 10 keV onboard ASCA and BeppoSAX (e.g. Ueda et al. 1999; Fiore et al. 1999). The main problem with these pilot surveys is the error boxes at fluxes close to the limit, whose size left substantial uncertainties on the optical identification, especially for the type 2 AGN (see La Franca et al. 2002, for a discussion on this point). The situation improved greatly in the last four years thanks to Chandra and XMM-Newton, both of which image the sky up to 10 keV with much higher sensitivity and much better angular resolution (at the arcsecond level in the case of Chandra). The combination of these two qualities have led to positionally based identifications, followed by spectroscopic identifications of the counterparts, which are regarded as fairly secure down to magnitudes  $R$  about 24. The X-ray flux limit achieved with a high fraction of identified sources is approximately  $10^{-15}$  erg cm $^{-2}$  s $^{-1}$  (e.g. La Franca et al. 2005). With the instrument sensitivity covering the spectra down to 0.5 keV, along with the knowledge of  $z$ , it is possible to estimate both the intrinsic value of  $N_{\text{H}}$  and the X-ray luminosity  $L_{\text{x}}$  corrected for absorption. After accumulating a sufficiently large sample to cover the  $L_{\text{x}} - z$  plane, one can investigate simultaneously the

X-ray luminosity function of AGN (irrespective of their being optically classified as type 1 or 2), its cosmic evolution, and the distribution of  $N_{\text{H}}$  as a function of  $L_{\text{x}}$  and  $z$ . In the following,  $L_{\text{x}}$  will be referred to as the intrinsic luminosity in the 2–10 keV band. As noted in Sect. 1, truly Compton-thick sources remain basically unsampled, thus the constraint emerging from these studies apply only to sources with  $N_{\text{H}}$  ranging from (nominally) zero to about  $10^{24} \text{ cm}^{-2}$ . With the statistics achieved so far it appears premature to observationally quantify the functional form of the  $N_{\text{H}}$  distribution. At present it is convenient to adopt a conservative approach, by using the ratio  $\xi = (\text{number of sources with } \log(N_{\text{H}}) > 22) / (\text{total number of sources})$ . Ueda et al. (2003) have shown that  $\xi$  is dependent on  $L_{\text{x}}$ , that is  $\xi = \xi(L_{\text{x}})$ , where  $\xi$  decreases with increasing  $L_{\text{x}}$ . Moreover, the same authors reached the conclusion that this property appears to be quantitatively independent from  $z$ . Recently, with a larger sample, which overlaps the one utilized by Ueda et al. (2003), but yields a wider coverage of the  $L_{\text{x}} - z$  plane, La Franca et al. (2005) confirmed the first finding, but not the second. Namely they find evidence of a  $z$  dependence, thus formally  $\xi = \xi(L_{\text{x}}, z)$ , where  $\xi$  increases and becomes shallower as  $z$  increases.

In this paper only the dependence of  $\xi$  on  $L_{\text{x}}$  in the local universe, as obtained by La Franca et al. (2005) from  $z = 0$  to  $z = 0.1$ , will be used as the novel constraint, while the dependence on  $z$  will be briefly commented upon and left as the subject of further investigations.

The next section is devoted to investigate whether this anticorrelation can be understood in the frame of physical models of the torus.

### 3. The case of the “thick torus”

Several authors (Krolik & Begelman 1986, 1988; Beckert & Duschl 2004; Vollmer et al. 2004; Beckert et al. 2004) have addressed in physical terms the dynamical and geometrical structure of the “thick torus”, which is assumed to be cylindrically symmetric. If  $R$  is the distance from the AGN centre (the site of the black hole, BH, with mass  $M_{\text{BH}}$ ), and  $H(R)$  is the scale height (vertical geometrical thickness), these models are often depicted (see Fig. 1) as if the “torus” were sharply confined within  $2H(R)$ , with all the obscuring matter within and nothing outside. This type of descriptive picture applies well to the separation of the Compton-thick sources from the rest. One could imagine a smoother transition of the obscuring matter density, in order to accommodate also the absorbed, but Compton-thin sources. The question is then the following: do these models, on the grounds of their physical principles and self-consistency, behave in a way that, without additional ad hoc assumptions, comply with the constraints described in Sect. 2? In these models  $H$  is an increasing function of  $R$ , simply as a consequence of the gravity exerted by the BH, in addition to that exerted by a concentric and, in first approximation, spherically symmetric stellar structure. In order to ensure the required scaleheight together with the most effective obscuration, the matter is assumed to be in the form of dense molecular clouds, endowed with the adequately large velocity dispersion. The clouds are considered to be either self-gravitating (Beckert & Duschl 2004; Vollmer et al. 2004) or in pressure

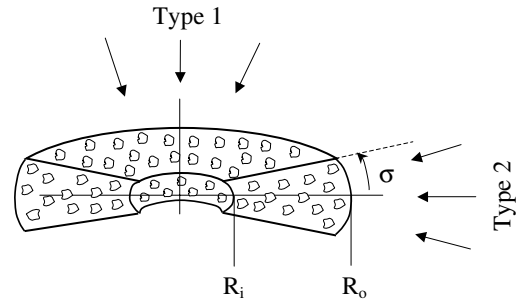


Fig. 1. Geometry of the “thick torus” (Nenkova et al. 2002).

equilibrium with a hot phase. The clouds can closely interact with each other or be subject to tidal shear, both effects leading to their destruction: they set stringent limits on the cloud size (hence their internal density) as well as on their number density as a function of  $R$ . Beckert et al. (2004) have shown that the geometrical thickness of the torus is given by:

$$H = \sqrt{\frac{2R^3 \dot{M}}{c_s M(R)}} \quad (1)$$

where  $\dot{M}$  is the total mass accretion rate,  $M(R)$  the mass within the radius  $R$  and  $c_s$  is the sound speed.

In order to maintain the obscuration effective as required by observations (see Sect. 1),  $\dot{M}$  must be much larger than  $\dot{M}_{\text{Edd}}$ , namely most of the matter contributing to  $\dot{M}$  must be lost, and only a fraction of it ( $\dot{M}_{\text{lum}}$ ) is allowed to feed the AGN power (see Fig. 4 in Beckert & Duschl 2004.). If  $\dot{M}_{\text{lum}}$  increases with  $\dot{M}$ , which seems reasonable to assume,  $H/R$ , hence the covered fraction of  $4\pi$ , would increase with the luminosity, contrary to the novel constraint.

One might of course read this conclusion as suggesting that something, to be physically demonstrated, is acting in the system to ensure anticorrelation between  $\dot{M}$  and  $\dot{M}_{\text{lum}}$ . So far no account has been taken of the feedback on the state of the matter due to the irradiation by the AGN itself. The ionization-evaporation effects set a limit on the minimum distance to which an absorbing cloud can survive. A useful quantification follows (Krolik & Begelman 1988) from equating the “evaporation time-scale” and the “accretion time-scale”:

$$R_{\text{evap}} = \frac{0.79 M_{\text{gas},5} L_{44}}{\dot{M}_{\text{torus}} R_{\text{out}} N_{\text{cl},24} T_5^{1/2}} \text{ pc} \quad (2)$$

where  $L_{44}$  is the central ionizing luminosity in units of  $10^{44} \text{ erg s}^{-1}$ ,  $M_{\text{gas},5}$  is the gas mass in units of  $10^5 M_{\odot}$ ,  $N_{\text{cl},24}$  is the column density of a single cloud in units of  $10^{24} \text{ cm}^{-2}$ ,  $T_5$  is the temperature at the sonic point of the evaporating flow in units of  $10^5 \text{ K}$ , and  $R_{\text{out}}$  is the outer radius of the configuration. In a purely geometrical model of the “torus”, described as a cylinder with a cavity (Lawrence 1991), the radius of the latter is bound to increase with the luminosity. Consequently, the covered fraction of  $4\pi$  would decrease. However this would be an acceptable answer to the anticorrelation described in Sect. 2 if one were able to demonstrate that physically  $H/R$  can be maintained constant (or decrease) versus  $R$ . The physical models summarized above, if  $M(R)$  increases with  $R$  less than linearly (as it is the case when this term is dominated by the

BH mass) show instead that the pure effect of the BH gravity involves a concave geometry (see Fig. 3 in Beckert & Duschl 2004), hence the covered fraction is basically determined by  $H$  at  $R_{\text{out}}$ . This implies that the fraction of obscured sources would be independent of the luminosity up to a certain value at which the illumination is so strong to forbid the formation of the torus. This is thence an on-off effect, which could be relevant to the issue of the fraction of Compton-thick sources as a function of their luminosity: this issue at present lacks an observationally secure point of reference, and will not be further discussed in this paper.

#### 4. Obscuration by molecular gas in the galactic disk

On the basis of a statistical analysis of the correlation between the spectroscopic optical classification of nearby AGN and the inclination to the line of sight of the host (typically spiral) galaxies, Maiolino & Rieke (1995) found the following. For the extreme type 2 there seems to be no correlation. On the contrary, types 1+1.2+1.5 are mostly found in face-on galaxies, and the intermediate types, 1.8+1.9, are mostly found in edge-on galaxies. They therefore suggested that the obscuration in the intermediate AGN types is associated with the gas in the galactic disks. Risaliti et al. (1999) showed that these types, when observed in X-rays, correspond to Compton-thin AGN.

It remains to be seen if the anticorrelation discussed in Sect. 2. could be explained within this scheme. The gas content at large in the disk of spiral galaxies correlates with their morphological type. In particular, the *mean* HI surface density over the disk out to the same isophotal radius is about twice in Sc than in Sa galaxies (Roberts & Haynes 1994). However, the concentration of the gas is generally associated with the spiral arms. So, it should increase towards the center in the Sa type, where the arms are more tightly wound, and decrease in later types. Furthermore, since the far infrared emission (FIR) appears to correlate with the CO flux, thus with the molecular gas content, it is noteworthy that the *mean* FIR surface density declines slightly from the Sa to the Sc type (Roberts & Haynes 1994). It should be therefore a fair approximation to assume that the relevant, HI + H<sub>2</sub>, gas content in the innermost, say 0.5 kpc scale, region is not significantly (for our purpose) dependent on the morphological type. On the other hand, along the sequence Sa-Sc, the bulge component relative to the disk is largest in the earliest type and decreases thence. In addition, there exist a fairly close relationship between bulge luminosity and central BH mass (Ferrarese & Ford 2005). Thence, if the AGN  $L_x$  were (statistically) correlated with  $M_{\text{BH}}$ , one should not expect the existence of the trend given by  $\xi(L_x)$ .

This statement follows, of course, only if one refers to the gas content alone, and the gravitational influence of the BH (and the bulge) on the geometrical thickness of the gas within the first few hundred parsec from the center is disregarded. In the following, it is argued that this influence might indeed shed some light on the anticorrelation that one would like to explain. To illustrate the point, an “idealized” design is adopted, where the molecular gas is confined within a self-gravitating, starry

galaxy disk, whose surface density  $\Sigma$  remains practically constant within a distance from the center of the order of one kpc. The scale height  $H_c$  of the molecular clouds is regulated by the disk gravity and their velocity dispersion. When closing inwards, the bulge and the BH gravity adds to that of the starry disk, inducing a progressive shrinking of  $H_c$ . In geometrical terms this picture is quite similar to the one which applies to the physical models of the torus, summarized in the previous section. In physical terms it is simpler, because outside a certain radial distance the collisional and tidal effects have no serious impact and can be disregarded.

The picture is characterized by the following parameters.

- The number density  $n_0$  of the clouds at  $Z = 0$ .
- The scale height defined according to

$$n(Z) = n_0 e^{-\left(\frac{Z}{H_c}\right)}. \quad (3)$$

- The clouds idealized as single spherical entities. Those which matter most for the absorption have the largest mass, i.e. the clouds that in our Galaxy dominate the mass function (where most of the mass resides). Thus single values for mass, radius, internal density are used:  $m_c$ ,  $r_c$ ,  $\rho_c$ . Further parameters are the velocity dispersion  $\sigma$  and the internal temperature  $T_c$ .
- The clouds are assumed to be in pressure equilibrium with an external gas (namely  $m_c < m_{\text{jeans}}$ ), whose  $\rho_e$  and  $T_e$  are such that  $\rho_e T_e = \rho_c T_c$ , and  $H_e \propto H_c T_e / \sigma > H_c$ .

Within at most 1 kpc both  $H_c$  and  $H_e$  are assumed constant and regulated by the disk force per unit mass,  $K_Z$ .

In this section, the gravitational effects of a central BH (and the related Bulge mass) are described. Down to where, along  $R$ , it can be assumed (lacking obvious reasons to the contrary) that  $\sigma_c$  and  $T_e$  remain constant (as well as the Bulge density), this addition shall result into a change in  $H_c$ , namely this quantity will decrease with decreasing  $R$ , as soon as the vertical attraction exerted by the BH will start dominating. The profile  $H_c(R)$  will go through an inflection at  $R_{\text{infl}}$ , which regulates the cone opening angle, and increases with  $M_{\text{BH}}$ . Thus, if there were a statistical correlation between  $M_{\text{BH}}$  and  $L_x$ , the consequence would be a trend of the type given in Sect. 2, which is encouraging.

The force per unit mass exerted in the vertical,  $Z$ , direction by the matter in the disk can be expressed, within about  $Z = 100$  pc, as

$$K_{Z,d} = -4\pi G \rho_d Z \quad (4)$$

where  $\rho_d$  is the approximately constant density of the matter in the disk, mainly provided by stars.

The equivalent force exerted by the BH, in the approximation  $Z \ll R$ , is given by

$$K_{Z,\text{BH}} = -G \frac{M_{\text{BH}}}{R^3} Z. \quad (5)$$

Similarly, the force exerted by the Bulge is

$$K_{Z,b} = -G \frac{M_b(R)}{R^3} Z = -G \frac{4\pi \rho_b}{3} Z \quad (6)$$

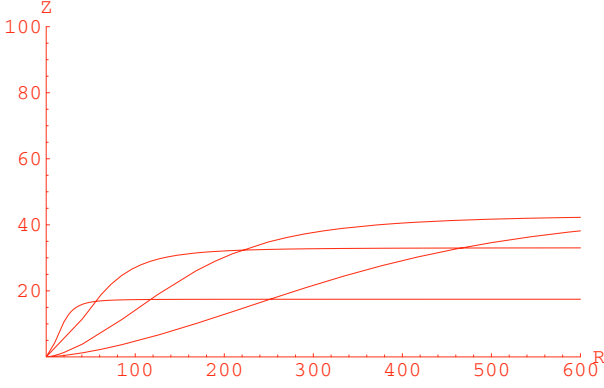


**Fig. 2.** Scale height of the clouds as a function of  $R$  when  $M_{\text{BH}} = 10^6 M_{\odot}$ ,  $10^7 M_{\odot}$ ,  $10^8 M_{\odot}$  and  $10^9 M_{\odot}$ .

where  $M_{\text{b}}(R)$  is the bulge mass within the radius  $R$ . We have assumed a spherical symmetry, and a constant bulge density  $\rho_{\text{b}}$  within  $R$  (see the Appendix, where  $\rho_{\text{b}}$  is calculated as a function of the Black Hole mass).

From the equation that links the clouds velocity dispersion and scale height to the sum of the three contributions to  $K_{\text{Z}}$

$$\sigma^2 = 2 \int_{H_{\text{c}}}^0 (K_{\text{Z,d}} + K_{\text{Z,BH}} + K_{\text{Z,b}}) dZ \quad (7)$$

one infers

$$H_{\text{c}}(R) = \left( \frac{\sigma^2}{4\pi G \rho_{\text{d}} + \frac{GM_{\text{BH}}}{R^3} + \frac{4\pi G \rho_{\text{b}}}{3}} \right)^{1/2}. \quad (8)$$

The distance of the point of inflection is then immediately derived to be

$$R_{\text{infl}} = \frac{1}{2} \left( \frac{M_{\text{BH}}}{4\pi \rho_{\text{d}} + \frac{4\pi \rho_{\text{b}}}{3}} \right)^{1/3}. \quad (9)$$

To be noted that at  $R = 2R_{\text{infl}}$  the gravitational pull of the BH in the  $Z$  direction is equal to that of the matter in the disk and the bulge. For values of  $R$  much lower than  $2R_{\text{infl}}$ , where the BH dominates, we shall disregard the contribution of the shrinking disk gravity (that is the increase of  $\rho_{\text{d}}$  with decreasing  $R$ ), and the profiles of  $H_{\text{c}}$  shown in Fig. 2 correspond to a choice of  $\rho_{\text{d}}$  equal to the value typical of a galaxy like our own, namely  $0.84$  solar masses per cubic parsec, a velocity dispersion  $\sigma = 10 \text{ km s}^{-1}$ , and four values of  $M_{\text{BH}}$  (and thence of  $\rho_{\text{b}}$ ). The opening angle is very sensitive to the last parameter, and depends on the value of  $R_{\text{infl}}$  increasing from  $12 \text{ pc}$  when  $M_{\text{BH}} = 10^6 M_{\odot}$  to  $226 \text{ pc}$  when  $M_{\text{BH}} = 10^9 M_{\odot}$ .

In order to evaluate the effective obscuration, this geometrical effect must be accompanied by assumptions on the number of clouds along a line of sight. To this end, the vertical distribution of the clouds number density is assumed to follow an exponential law

$$n(Z, R) = n_0(R) e^{-\left(\frac{Z}{H_{\text{c}}(R)}\right)} \quad (10)$$

where  $H_{\text{c}}(R)$  is given by Eq. (8) and  $n_0$  is defined through the surface density  $\Sigma$ , assumed constant with  $R$ :

$$\Sigma = 2M_{\text{c}} \int_0^{\infty} n_0(R) e^{-\left(\frac{Z}{H_{\text{c}}(R)}\right)} dZ \quad (11)$$

**Table 1.** Adopted values for the parameters. See text for details.

Disk matter density	$\rho_{\text{d}} = 0.84 M_{\odot} \text{ pc}^{-3}$
Clouds velocity dispersion	$\sigma = 10 \text{ km s}^{-1}$
Scale height of the clouds	$H_{\text{c}} = 50 \text{ pc}$
Typical cloud inner density	$\rho_{\text{c}} = 10^4 \text{ cm}^{-3}$
Typical cloud radius	$r_{\text{c}} = 0.167 \text{ pc}$
Typical cloud column density	$N_{\text{H,c}} = 10^{22} \text{ cm}^{-2}$
Typical cloud mass	$M_{\text{c}} = 4.35 M_{\odot}$
Typical cloud temperature	$T_{\text{c}} = 10 \text{ K}$
External gas temperature	$T_{\text{e}} = 10^6 \text{ K}$
External gas density	$\rho_{\text{e}} = 0.1 \text{ cm}^{-3}$
Cloud number density at $z = 0$	$n_0 = \Sigma / 2H_{\text{c}} M_{\text{c}}$
Tidal radius $R$ for $M_{\text{BH}} = 10^9 M_{\odot}$	$R_{\text{tidal}} = 128 \text{ pc}$
Tidal radius $R$ for $M_{\text{BH}} = 10^8 M_{\odot}$	$R_{\text{tidal}} = 60 \text{ pc}$
Tidal radius $R$ for $M_{\text{BH}} = 10^7 M_{\odot}$	$R_{\text{tidal}} = 28 \text{ pc}$
Tidal radius $R$ for $M_{\text{BH}} = 10^6 M_{\odot}$	$R_{\text{tidal}} = 13 \text{ pc}$
Inflection radius $R$ for $M_{\text{BH}} = 10^9 M_{\odot}$	$R_{\text{infl}} = 226 \text{ pc}$
Inflection radius $R$ for $M_{\text{BH}} = 10^8 M_{\odot}$	$R_{\text{infl}} = 101 \text{ pc}$
Inflection radius $R$ for $M_{\text{BH}} = 10^7 M_{\odot}$	$R_{\text{infl}} = 39 \text{ pc}$
Inflection radius $R$ for $M_{\text{BH}} = 10^6 M_{\odot}$	$R_{\text{infl}} = 12 \text{ pc}$

where  $M_{\text{c}}$  is the mass chosen to represent the single cloud. Thus:

$$n(Z, R) = n_0 \frac{H_{\text{c}}}{H_{\text{c}}(R)} e^{-\left(\frac{Z}{H_{\text{c}}(R)}\right)}, \quad (12)$$

where  $H_{\text{c}}$  is the scale height at  $R \gg R_{\text{infl}}$ . Except for the parameter  $\Sigma$ , all the other adopted quantities are given in Table 1. In this table also a tidal radius is given, namely the distance within which the single cloud would be disrupted by the tidal force exerted by the BH, namely

$$R_{\text{tidal}} = \left( \frac{3M_{\text{BH}}}{2\pi\rho_{\text{c}}m_{\text{H}}} \right)^{1/3}, \quad (13)$$

where  $\rho_{\text{c}}$  is the internal density of the cloud, assumed equal to  $10^4$  hydrogen molecules  $\text{cm}^{-3}$ . It should be noted that  $R_{\text{tidal}}$  is of the same order of  $R_{\text{infl}}$  for a BH mass of  $10^6 M_{\odot}$ , and lower for higher masses. The adopted cloud size is such that the corresponding column density is equal to  $10^{22} \text{ cm}^{-2}$ . Because this is the value of  $N_{\text{H}}$  chosen to discriminate between Seyferts with no absorption and Compton–thin absorbed ones, we have then simply to calculate the probability that one single cloud happens to lie along the line of sight. It is easy to demonstrate that it does not make a difference if such clouds, or smaller ones, where congregated in complexes rather than dispersed, as assumed, provided that the number of complexes remains large.

The line of sight is defined through the angle  $\theta$  given by

$$\frac{Z}{R} = \text{tg}\theta, \quad (14)$$

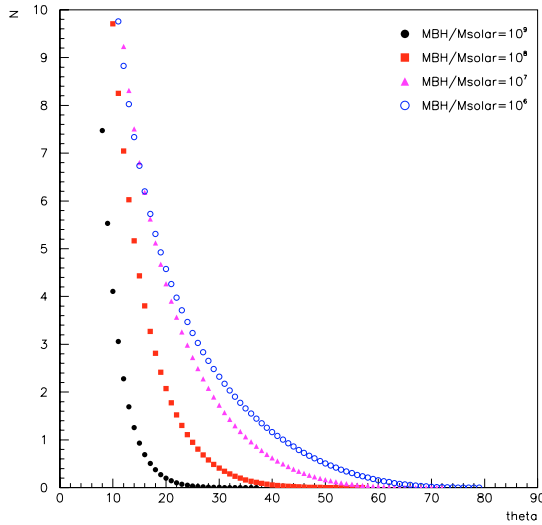


**Fig. 3.** Number of clouds along the line of sight as a function of  $\theta$  for four values of  $M_{\text{BH}}$ , when  $\Sigma = 200 M_{\odot} \text{pc}^{-2}$ .

and the number density as a function of  $\theta$  and  $R$  obtains from Eq. (12):

$$n(\theta, R) = n_0 \frac{H_c}{H_c(R)} e^{-\left(\frac{R \sin \theta}{H_c(R)}\right)}. \quad (15)$$

For a given  $\theta$  the number of encountered clouds is given by

$$N = \pi r_c^2 \int_{R_{\text{in}}}^{R_{\text{out}}} n(\theta, R) dR, \quad (16)$$

where  $\pi r_c^2$  is the geometric cross section of a cloud,  $R_{\text{out}} = 4H_c/\tan \theta$  and  $R_{\text{in}}$  is consistently adopted equal to  $R_{\text{tidal}}$ .

Figure 3 illustrates the number of clouds encountered as a function of  $\theta$ , for four values of the  $M_{\text{BH}}$  and  $\Sigma$  equal to  $200 M_{\odot} \text{pc}^{-2}$ .

By defining  $\theta_*$  as the angle where this number equals 1, it is straightforward to estimate the solid angle, hence the fraction of sources  $N_s$  where the line of sight is bound to cross a column of at least  $10^{22} \text{cm}^{-2}$ ,

$$\frac{N_s (\log N_{\text{H}} > 22)}{N_{s, \text{tot}}} = \cos(90 - \theta_*) \quad (17)$$

as a function of two parameters, the BH mass and the surface density  $\Sigma$  of the molecular gas within  $R_{\text{out}}$ .

In Fig. 4 (left panel), the fraction of absorbed AGN is shown for four different values of the BH mass ( $10^6$ ,  $10^7$ ,  $10^8$  and  $10^9 M_{\odot}$ ) and several choices of  $\Sigma$ . In order to draw a comparison with the observational evidence, where the observable is the X-ray luminosity, it is necessary to adopt a relation between  $L_x$  and  $M_{\text{BH}}$ . The luminosity-dependent bolometric correction in Marconi et al. (2004; see their Eq. (21) and Fig. 3) and a luminosity at 0.1 times the Eddington limit (see e.g. Peterson et al. 2004) have been adopted. The results are given in Fig. 4 (right panel), where the best-fit relationship between the fraction of absorbed AGN and X-ray luminosity obtained by La Franca et al. (2005) is shown for comparison.

The dependence of the slope of the anticorrelation on the adopted value of  $\Sigma$  is noteworthy. While for values of this parameter larger than about  $80\text{--}100 M_{\odot} \text{pc}^{-2}$  the slope changes

rather little, and remains gratifyingly close to the observed one, for smaller values it becomes shallower, and the more so the lower the value. This comes out simply because, in order to intercept a cloud, one needs to integrate well beyond the inflection radius: in other words, despite the shrinking in  $H_c$  due to the black hole, the number density remains too small to have any sizeable effect within  $2R_{\text{infl}}$ , and the required absorption is obtained only for line of sights grazing the plane of the disk.

## 5. Discussion and conclusions

The main result of this paper is that the anticorrelation between  $\xi(L_x)$  (namely the fraction of AGN with  $N_{\text{H}}$ , as measured by their X-ray spectra, greater than  $10^{22} \text{cm}^{-2}$ ) and  $L_x$  in Compton-thin objects is at least qualitatively reproduced provided that: a) there is a sufficiently large number of molecular clouds within the radius where the BH gravitational influence is dominant; b) there is, in a statistical sense, a correlation between the BH mass and the AGN luminosity. These two conditions are now briefly discussed.

As shown in Fig. 4, the slope and the normalization of the anticorrelation are consistent with the observational results for values of  $\Sigma \geq 150\text{--}200 M_{\odot} \text{pc}^{-2}$ , if a bolometric luminosity 0.1 times the Eddington luminosity is assumed (as it seems to be the case in the local universe, e.g. Peterson et al. 2004). Thus, the first question arising is what are the typical values of this quantity in the innermost region of spiral galaxies (the hosts of Seyfert active nuclei). The relevant radius of this region,  $2R_{\text{infl}}$ , lies between about 25 and 450 pc (for  $M_{\text{BH}}$  from one and one thousand million solar masses), which corresponds to 0.5–9 arcsec at a distance of 10 Mpc, and requires the best angular resolution currently achievable, with interferometry at the 3 mm CO  $J = 1\text{--}0$  line, on relatively nearby galaxies. In this respect, the BIMA Survey of Nearby Galaxies (BIMA SONG) at Hat Creek, CA, with the 10-element Berkeley-Illinois-Maryland Association (BIMA) millimeter interferometer (Helfer et al. 2003) is the best available for our purpose, because the sample was deliberately selected without reference to CO or infrared brightness. It consists of 44 spiral galaxies of all morphological types (the Sa type are somewhat undersampled relative to the later types). The angular resolution of 6 arcsec corresponds to 360 pc (that is 180 pc radius for the central region) at the average distance of the galaxies, 12 Mpc. From the CO surface brightness distribution (see Table 5 in Helfer et al. 2003) it turns out that the peak brightness is attained within the central 6 arcsec in 20 out of 44 galaxies. In these 20 objects the corresponding surface density  $\Sigma_{\text{centr}}$  lies between 15 and  $1854 M_{\odot} \text{pc}^{-2}$ , with most of them (18) above 90, and the other two around  $15 M_{\odot} \text{pc}^{-2}$ . Notably, among the other 24 galaxies, 10 have  $\Sigma_{\text{centr}} \geq 50 M_{\odot} \text{pc}^{-2}$ , with values up to 1151. The galaxies with  $\Sigma_{\text{centr}} \geq 150 M_{\odot} \text{pc}^{-2}$  are 22/44, namely 50%. The straight mean value of this 22 galaxies is  $511 M_{\odot} \text{pc}^{-2}$ , notably close to the value of  $\sim 500 M_{\odot} \text{pc}^{-2}$  of the 300 pc molecular disk in our own galaxy (Güsten 1989).

The sample contains 8 objects classified as Seyfert galaxies, 6 of them with  $\Sigma_{\text{centr}}$  greater than 90 and up to  $466 M_{\odot} \text{pc}^{-2}$ , 1 (NGC 4725) with  $\Sigma_{\text{centr}} = 21 M_{\odot} \text{pc}^{-2}$ , 1 (NGC 3031) with



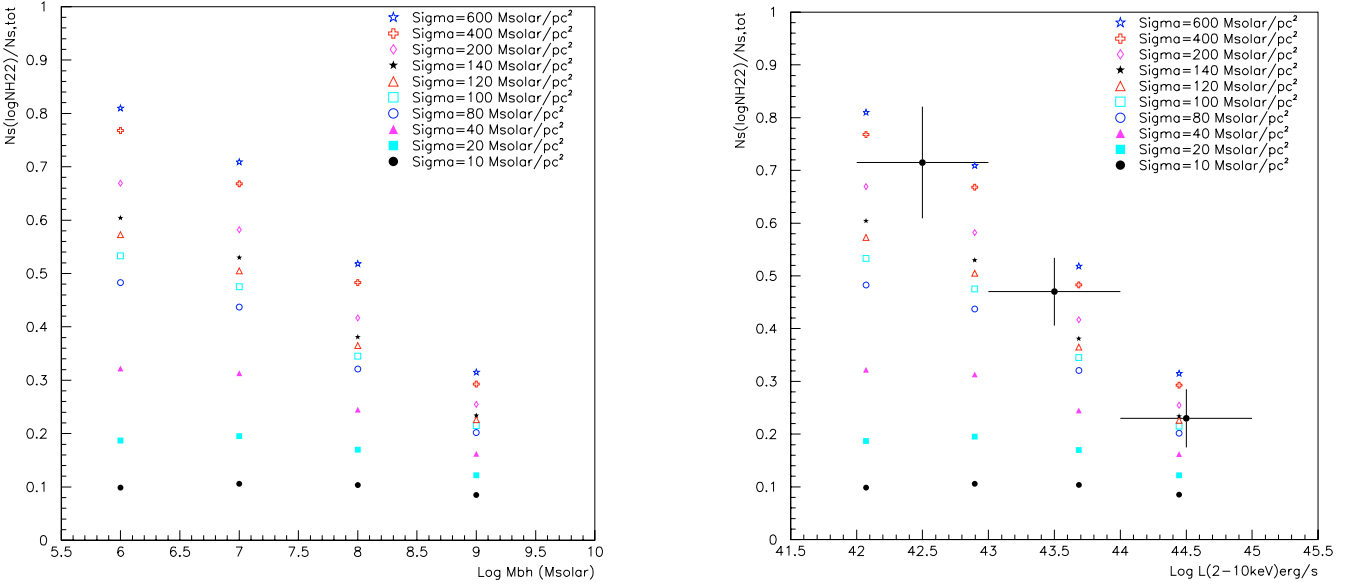


**Fig. 4.** Expected behaviour of the fraction  $N_s(\log N_H > 22)/N_{s,\text{tot}}$ , for several values of  $\Sigma$ , as a function  $M_{\text{BH}}$  (*left hand panel*) and of  $L(2-10 \text{ keV})$  (*right hand panel*), with the latter derived assuming  $L_{\text{Bol}}/L_{\text{Edd}} = 0.1$  (e.g. Peterson et al. 2004) and the luminosity-dependent bolometric correction in Marconi et al. (2004). In the right hand panel, crosses represent the observed fraction (corrected for selection effects, and adapted from La Franca et al. 2005) of obscured AGN in the local universe.

$\Sigma_{\text{centr}}$  below the detection limit: the proportion of galaxies with an active nucleus, which possess a high value of  $\Sigma_{\text{centr}}$ , appears to be, within the small statistics, similar to that in the general population.

The fraction of objects which meet our requirements is encouraging, especially because it does not require a special correlation with the nuclear activity, and represents a relatively large scale (compared to the close circumnuclear environment) property fairly common in spiral galaxies. In other words, the condition required is already in place in about half of the galaxies before a high rate nuclear activity lights up, which in turn is unlikely to significantly influence the preexisting condition. Much higher resolution and sensitivity surveys are needed to explore more distant objects, and therefore draw more solid conclusions on the validity of our hypothesis: to pursue this goal an array of millimeter telescopes like ALMA is necessary.

Concerning the increase of the fraction of absorbed sources with redshift (La Franca et al. 2005), an interesting possibility is that it might be due to an average increase of  $\dot{M}$  with the redshift, if one were allowed to assume that the molecular content and distribution in spiral galaxies is independent of  $z$ . Indeed, McLure & Dunlop (2004) found that the  $L_{\text{bol}}/L_{\text{Edd}}$  ratio raises from about 0.15 at  $z \sim 0.2$  to 0.5 at  $z \sim 2$ . We intend to investigate this issue further, in particular within the frame of astrophysically self consistent models, which associate the growth of the supermassive BH in galaxies with the evolution in cosmic time of the AGN population (e.g. Menci et al. 2004).

*Acknowledgements.* The authors are grateful to Renzo Sancisi and Roberto Maiolino for useful discussions and for their help in exploring the literature on the CO central concentration in galaxies. They thank the referee for his constructive comments. They acknowledge financial support from ASI and MIUR (under grant PRIN-02-02-23).

## Appendix A: Effects of the stellar bulge

The BH mass is known to correlate with the velocity dispersion,  $\sigma_b$ , in the bulge:

$$\frac{M_{\text{BH}}}{10^8 M_{\odot}} = (1.66 \pm 0.24) \left( \frac{\sigma_b}{200 \text{ km s}^{-1}} \right)^{\alpha}, \quad (\text{A.1})$$

with  $\alpha = 4.86 \pm 0.43$  (Ferrarese & Ford 2005).

With respect to the virial mass of the bulge

$$GM_b \approx \sigma_b^2 R_b, \quad (\text{A.2})$$

the BH mass turns out (Merritt & Ferrarese 2001) proportional to  $M_b$ ,  $M_{\text{BH}} \approx 10^{-3} M_b$ . From Eqs. (A.1) and (A.2) one immediately obtains

$$R_b \propto \frac{M_b}{\sigma_b^2} \propto \frac{M_{\text{BH}}}{M_{\text{BH}}^{2/\alpha}} \propto M_{\text{BH}}^{1-2/\alpha}, \quad (\text{A.3})$$

or, rounding off  $\alpha$  to 5,

$$R_{\text{bulge}} \propto M_{\text{BH}}^{3/5}. \quad (\text{A.4})$$

Adopting for the density profile of the bulge the relationship:

$$\rho(R) = \frac{\rho_b}{1 + (R/R_c)^2} \quad (\text{A.5})$$

where  $\rho_b$  is the central density and  $R_c$  is the core radius, if it is assumed that  $R_c$  is proportional to  $R_b$ , it follows that  $R_c \propto M_{\text{BH}}^{3/5}$ . After normalization to the values which apply to the Milky Way, namely  $R_{c,\text{MW}} = 400 \text{ pc}$ ,  $M_{\text{BH},\text{MW}} = 4 \times 10^6 M_{\odot}$ , one obtains:

$$\begin{aligned} M_{\text{BH}} &= 10^6 M_{\odot} & R_c &= 180 \text{ pc} \\ M_{\text{BH}} &= 10^7 M_{\odot} & R_c &= 700 \text{ pc} \\ M_{\text{BH}} &= 10^8 M_{\odot} & R_c &= 2.7 \text{ kpc} \\ M_{\text{BH}} &= 10^9 M_{\odot} & R_c &= 11 \text{ kpc}. \end{aligned}$$

For these values of  $M_{\text{BH}}$   $R_c$  turns out to be much larger than two times  $R_{\text{infl}}$  defined in Sect. 4 and given in Table 1. Thus it can be concluded that the stellar bulge density within  $2R_{\text{infl}}$  remains practically constant. Its value, in the above approximations, is proportional to  $M_{\text{BH}}^{-4/5}$ , and we calculated it for each BH mass by simply rescaling the Milky Way value:

$$M_{\text{BH}} = 10^6 M_{\odot} \quad \rho_b = 15.1 M_{\odot}/\text{pc}^3$$

$$M_{\text{BH}} = 10^7 M_{\odot} \quad \rho_b = 2.4 M_{\odot}/\text{pc}^3$$

$$M_{\text{BH}} = 10^8 M_{\odot} \quad \rho_b = 0.4 M_{\odot}/\text{pc}^3$$

$$M_{\text{BH}} = 10^9 M_{\odot} \quad \rho_b = 0.06 M_{\odot}/\text{pc}^3.$$

## References

- Antonucci, R. R. J. 1993, *ARA&A*, 31, 473  
 Antonucci, R. R. J., & Miller, J. S. 1985, *ApJ*, 297, 621  
 Beckert, T., & Duschl, W. J. 2004, *A&A*, 426, 445  
 Beckert, T., Duschl, W. J., & Vollmer, B. 2004, in *Growing Black Holes*, ed. A. Merloni, S. Nayakshin, & R. Sunyaev (Springer-Verlag), in press [arXiv:astro-ph/0410368]  
 Brandt, W. N., & Hasinger, G. 2005, *ARA&A*, in press [arXiv:astro-ph/0501058]  
 Comastri, A., Mignoli, M., Ciliegi, P., et al. 2002, *ApJ*, 571, 771  
 Elvis, M., Wilkes, B. J., & McDowell, J. C. 1994, *ApJS*, 95, 1  
 Ferrarese, L., & Ford, H. 2005, *SSRv*, 116, 523  
 Fiore, F., La Franca, F., Giommi, P., et al. 1999, *MNRAS*, 306, L55  
 Guainazzi, M., Matt, G., & Perola, G. C. 2005, *A&A*, 444, 119  
 Güsten, R. 1989, *The Center of the Galaxy*, IAU Symp., 136, 89  
 Hasinger, G. 2004, *Nucl. Phys. B Proc. Suppl.*, 132, 86  
 Helfer, T. T., Thornley, M. D., Regan, M. W., et al. 2003, *ApJS*, 145, 259  
 Ho, L., Filippenko, V., & Sargent, W. L. W. 1997, *ApJS*, 112, 315  
 Krolik, J. H., & Begelman, M. C. 1986, *ApJ*, 308, L55  
 Krolik, J. H., & Begelman, M. C. 1988, *ApJ*, 329, 702  
 La Franca, F., Fiore, F., Vignali, C., et al. 2002, *ApJ*, 570, 100  
 La Franca, F., Fiore, F., Comastri, A., et al. 2005, *ApJ*, in press [arXiv:astro-ph/0509081]  
 Lawrence, A. 1991, *MNRAS*, 252, 586  
 Maiolino, R., & Rieke, G. H. 1995, *ApJ*, 454, 95  
 Maiolino, R., Comastri, A., Gilli, R., et al. 2003, *MNRAS*, 344, L59  
 Malkan, M. A., Gorijn, V., & Tam, R. 1998, *ApJS*, 117, 25  
 Marconi, A., Risaliti, G., & Gilli, R. 2004, *MNRAS*, 351, 169  
 Matt, G. 2000, *A&A*, 355, L13  
 Matt, G. 2004, *Frontiers of X-ray Astronomy*, ed. A. C. Fabian, K. A. Pounds, & R. Blandford (Cambridge: Cambridge University Press), 175  
 Matt, G., Pompilio, F., & La Franca, F. 1999, *New Astr.*, 4, 191  
 McLure, R. J., & Dunlop, J. S. 2004, *MNRAS*, 352, 1390  
 Menci, N., Fiore, F., Perola, G. C., & Cavaliere, A. 2004, *ApJ*, 606, 58  
 Merritt, D., & Ferrarese, L. 2001, *ASPC*, 249, 335  
 Nenkova, M., Ivezić, Z., & Elitzur, M. 2002, *ApJ*, 570, L9  
 Perola, G. C., Matt, G., & Cappi, M. 2002, *A&A*, 389, 802  
 Peterson, B. M., Ferrarese, L., Gilbert, K. M., et al. 2004, *ApJ*, 613, 682  
 Piconcelli, E., Jimenez-Bailon, E., & Guainazzi, M. 2005, *A&A*, 432, 15  
 Risaliti, G., Maiolino, R., & Salvati, M. 1999, *ApJ*, 522, 157  
 Roberts, M. S., & Haynes, M. P. 1994, *ARAA*, 32, 115  
 Vollmer, B., Beckert, T., & Duschl, W. J. 2004, *A&A*, 413, 949  
 Ueda, Y., Takahashi, T., Ishisaki, Y., Ohashi, T., & Makishima, K. 1999, *ApJ*, 524, L11  
 Ueda, Y., Akiyama, M., Ohta, K., & Miyaji, T. 2003, *ApJ*, 598, 886  
 Weaver, K. A. 2001, in *The central kpc of starbursts and AGN: the La Palma connection*, ed. J. H. Knapen, J. E. Beckman, I. Shlosman, & T. J. Mahoney, *ASP Conf. Ser.*, 249, 389